

the Raman scattering experiment performed by Feldmann *et al.*<sup>9</sup>

The changes of the in-band mode frequencies of the longitudinal branch along the [001] direction were also measured and the results are shown in Fig. 3 together with the theoretical prediction (solid line). As the addition of 9.2% Si to Ge decreases the lattice constant by about 0.5%, the in-band mode frequencies should be expected to have a relative increase which is given approximately by  $\gamma(\Delta V/V)$ , where  $\gamma$  is the Grüneisen constant for the longitudinal branch and  $(\Delta V/V)$  is the relative change of the crystal volume. Using  $\gamma=1$ , an average value of the Grüneisen parameter as calculated by Dolling and Cowley,<sup>10</sup> the increase in the frequency due to the lattice contraction was estimated

and added to that calculated from the mass-defect theory. The resultant change is shown by the dotted line in the same figure. The over-all variation of the change as a function of the corresponding in-band mode frequency is qualitatively in good agreement with the experimental results, though the theory predicts a finer structure than that observed. This discrepancy may be due to the effects of the finite concentration that are not included in the theory. A change in the force constants may also have significant effects on the in-band mode frequencies. In order to examine this point further, an experiment on a Ge crystal with 5% Si will be performed in the near future.

We are grateful to G. Dolling for supplying the  $g(\nu)$  for pure Ge.

<sup>†</sup>Research sponsored by the U. S. Atomic Energy Commission under contract with Union Carbide Corporation.

<sup>1</sup>The crystal was kindly loaned by E. F. Hockings of RCA Laboratories to whom we are very grateful.

<sup>2</sup>J. P. Dismukes, L. Ekstrom, and R. J. Paff, *J. Phys. Chem.* **68**, 3021 (1964).

<sup>3</sup>B. N. Brockhouse and P. K. Iyengar, *Phys. Rev.* **111**, 747 (1958).

<sup>4</sup>G. Dolling, in *Inelastic Scattering of Neutrons in Solids and Liquids* (International Atomic Energy Agency, Vienna, 1963), Vol. II, p. 37.

<sup>5</sup>See, for example, A. A. Maradudin, *Solid State Phys.* **18**, 273 (1966).

<sup>6</sup>R. J. Elliott and D. W. Taylor, *Proc. Roy. Soc. (London)* **A296**, 161 (1967).

<sup>7</sup>D. W. Taylor, *Phys. Rev.* **156**, 1017 (1967).

<sup>8</sup>R. N. Aiyer, R. J. Elliott, J. A. Krumhansl, and P. L. Leath, *Phys. Rev.* **181**, 1006 (1969).

<sup>9</sup>D. W. Feldman, M. Ashkin, and J. H. Parker, Jr., *Phys. Rev. Letters* **17**, 1209 (1966).

<sup>10</sup>G. Dolling and R. A. Cowley, *Proc. Phys. Soc. (London)* **88**, 463 (1966).

## Transverse Negative Resistance in *n*-Type Germanium

Claes Hammar

*Microwave Institute, S-100 44 Stockholm 70, Sweden*

(Received 15 March 1971)

For *n*-type germanium the mobility in the [001] direction in the presence of a strong electric field in the [110] direction has been calculated using a detailed model of the material including higher  $\langle 100 \rangle$  minima. The method of calculation is a Monte Carlo approach capable of giving differential quantities. At room temperature no instability is found, while at 77°K an instability is obtained if the scattering rate between  $\langle 111 \rangle$  and  $\langle 100 \rangle$  minima is sufficiently strong.

### I. INTRODUCTION

It was first noted by Erlbach<sup>1</sup> that in *n*-type germanium a negative resistance might exist in a direction transverse to a strong electric field. The origin of this effect will be discussed in Sec. II. Erlbach found that this effect could be present in germanium only in a uniaxially stressed material. Shyam and Kroemer<sup>2</sup> measured a transverse polarization in *n*-type germanium at room temperature and interpreted this as an indication of the presence of the Erlbach effect. They explained this as a consequence of a strong repopulation induced by higher  $\langle 100 \rangle$  valleys.

A calculation of the resistance in the [001] direction in the presence of a strong electric field in the [110] direction is presented in this paper. The model of the material includes the effect of the  $\langle 100 \rangle$  valleys and is similar to the one used by Paige<sup>3</sup> in a study of the bulk negative conductivity in this material. This model was later used by the author<sup>4</sup> to calculate the anisotropy of the high-field conductivity with the Monte Carlo method. In Sec. III this method is generalized to give the differential conductivity. The numerical results are presented in Sec. IV. At room temperature no instability is found, while at 77°K the transverse resistance can be negative if the intervalley scattering rate be-

TABLE I. Conduction-band parameters of germanium, after Paige (Ref. 3).

Valley	No.	$m_L^*/m$	$m_T^*/m$	$\Delta$ (eV)
$\langle 111 \rangle$	4	1.577	0.0815	...
$\langle 000 \rangle$	1	0.037	0.037	0.14
$\langle 100 \rangle$	6	0.90	0.192	0.18

tween  $\langle 111 \rangle$  and  $\langle 100 \rangle$  valleys is sufficiently strong.

## II. PHYSICAL MODEL

The assumed values of the parameters characterizing the conduction band in germanium are given in Table I. In the model several approximations of the band structure are made. The  $\langle 000 \rangle$  minimum is neglected since there will be very few electrons in this valley due to the low effective mass. Furthermore, the nonparabolicity of the  $\langle 111 \rangle$  valleys is neglected. This effect is important only at rather high energies where there are few electrons if the coupling between  $\langle 111 \rangle$  and  $\langle 100 \rangle$  minima is strong. In analogy with silicon it is assumed that the intervalley scattering rate between  $\langle 100 \rangle$  valleys is strong. With this assumption it is a good approximation to neglect the anisotropy between the  $\langle 100 \rangle$  minima.

The assumed values of the scattering parameters are given in Table II. The acoustic scattering is approximated by an isotropic, velocity-randomizing collision process.<sup>5</sup> Furthermore, the energy relaxation by acoustic phonons is neglected, since it is only of importance at rather high energies where the energy relaxation due to nonequivalent intervalley scattering is strong.

In the calculations the ellipsoidal energy surfaces are transformed to spherical surfaces in the usual manner.<sup>6</sup> This means that each minimum is characterized by a certain electric field  $E^*$  with a magnitude dependent on the angle between the field and the symmetry axis of the energy ellipsoid. For a

general direction in the  $(1\bar{1}0)$  plane there are, in the model described above, four sets of nonequivalent minima. The Boltzmann equation in these minima is

$$\frac{eE_m^*}{\hbar} \frac{\partial f_m}{\partial k_L} + \nu f_m = \sum_{n=1}^4 L_{mn} f_n, \quad m=1, \dots, 4 \quad (1)$$

where  $f_m$  is the distribution function of the electrons in minimum  $m$ ,  $k_L$  the wave vector parallel to the field, and  $\nu$  the collision frequency.  $L_{mn}$  is an integral operator representing scattering into a volume element in momentum space.  $m=1$  corresponds to the  $\langle 111 \rangle$  minimum,  $m=2$  to the  $\langle 1\bar{1}\bar{1} \rangle$  minimum,  $m=3$  to the two equivalent minima  $\langle 1\bar{1}1 \rangle$  and  $\langle 1\bar{1}\bar{1} \rangle$ , and  $m=4$  to the six  $\langle 100 \rangle$  minima. In the case to be studied here, there is a strong electric field in the  $[110]$  direction and a small transverse field in the  $[001]$  direction. The effective fields can thus be written as  $E_m^* + \delta E_m^*$ . The relations

$$E_1^* = E_2^*, \quad (2)$$

$$\delta E_1^* = -\delta E_2^*, \quad (3)$$

and

$$\delta E_3^* = \delta E_4^* = 0 \quad (4)$$

are immediately obtained from the symmetry of the band structure. Writing the distributions as  $f_m + \delta f_m$ , Eq. (1) and relations (2)–(4) give

$$f_1 = f_2, \quad (5)$$

$$\delta f_1 = -\delta f_2, \quad (6)$$

and

$$\delta f_3 = \delta f_4 = 0. \quad (7)$$

With  $f_0 = f_1 + f_2$  and  $\delta f_0 = \delta f_1 - \delta f_2$  the equation for first-order quantities obtained from Eq. (1) is

$$\frac{eE_1^*}{\hbar} \frac{\partial \delta f_0}{\partial k_L} + \frac{e\delta E_1^*}{\hbar} \frac{\partial f_0}{\partial k_L} = (L_{11} - L_{12}) \delta f_0 - \nu \delta f_0. \quad (8)$$

TABLE II. Electron-phonon scattering processes in germanium, after Paige (Ref. 3).

Type	Minimum		Branch	Phonon energy (equiv temp) (°K)	$\bar{E}_{av}$ (eV)	$D$ (eV/m)
	Initial	Final				
Intravalley	111	111	acoustic	...	11.8	
	111	111	optic	430	...	$9 \times 10^{10}$
	100	100	acoustic	...	7.4	...
	100	100	optic	430	...	forbidden
Equivalent intervalley	111	$\bar{1}11$	acoustic	320	...	$1.6 \times 10^{10}$
	100	$\bar{1}00$	optic	430	...	$1.1 \times 10^{11}$
	100	$\bar{1}00$	acoustic	100	...	$8.8 \times 10^9$
	100	010	acoustic	320	...	$3.8 \times 10^{10}$
Nonequivalent intervalley	111	100	acoustic	320	...	$5 \times 10^{10}$

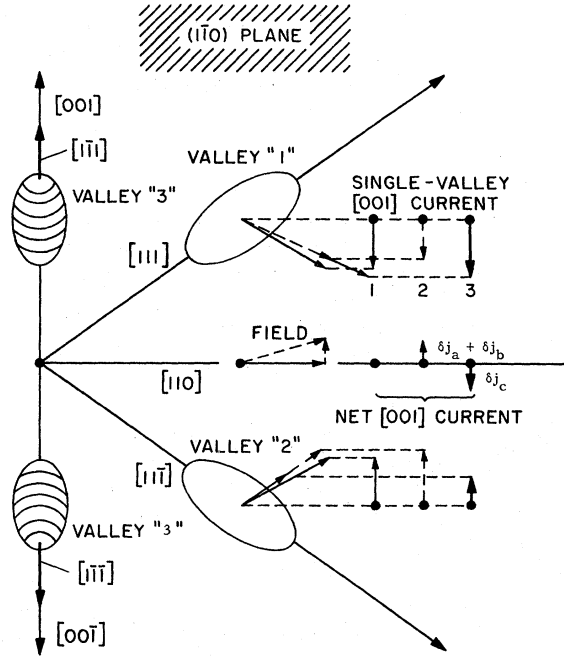


FIG. 1. Projection of the four  $\langle 111 \rangle$  valleys of Ge on the  $(1\bar{1}0)$  plane, together with the current contributions from the two valleys in that plane, for two field directions. Case 1 corresponds to a field exactly in the  $[110]$  direction, case 2 to a field tilted away from the  $[110]$  direction within the  $(1\bar{1}0)$  plane, but without electron redistribution between valleys 1 and 2. Case 3 includes this repopulation.

Thus, to the first order in the transverse field only the distributions in the  $\langle 111 \rangle$  and  $\langle 1\bar{1}\bar{1} \rangle$  minima are changed.

The transverse drift velocity can be separated into three components. This is best explained with the aid of Fig. 1. When the field  $\delta E$  is added, the directions of the drift velocities in all valleys will change. This gives a contribution  $\delta j_a$  to the current. In the  $\langle 111 \rangle$  and  $\langle 1\bar{1}\bar{1} \rangle$  valleys also the magnitude of the effective field is changed. For the direction of  $\delta E$  shown in Fig. 1 the effective field is decreased in the  $\langle 111 \rangle$  minimum and increased in the minimum  $\langle 1\bar{1}\bar{1} \rangle$ . Thus,  $v_2$  will increase and  $v_1$  decrease. This gives a contribution  $\delta j_b$  to the current. Carriers will also be redistributed from the  $\langle 111 \rangle$  to the  $\langle 1\bar{1}\bar{1} \rangle$  valley, resulting in a contribution  $\delta j_c$  to the transverse current.<sup>7</sup> If the repopulation effect is strong,  $\delta j_c$  will be larger than  $\delta j_a + \delta j_b$  and the transverse conductivity will be negative.

### III. MONTE CARLO APPROACH

The problem is to find a solution to Eq. (8). The conventional method is to assume a Maxwellian form of the distribution and solve for all parameters of interest. A comparison with Monte Carlo calculations<sup>8</sup> shows that this method tends to give

large errors in population ratios between different energy minima. Since the repopulation between valleys is of crucial importance for the existence of the Erlbach instability, it is obvious that Eq. (8) must be solved exactly. For this purpose two somewhat different Monte Carlo methods were developed. Both methods will be described below in a simple case for a single, isotropic valley with velocity-randomizing scattering processes.

The first method is based on the Monte Carlo method earlier used by the author<sup>4</sup> to calculate the anisotropy of the high-field conductivity in  $n$ -type germanium. In this method, the synchronous ensembles introduced by Price<sup>9</sup> were used. The "after-scattering" ensemble  $f_a$  is the distribution of particles immediately after they have been scattered. If collisions are velocity randomizing, then  $f_a$  will be spherically symmetric in momentum space and a function of energy only.  $f_a$  can be obtained from the transport equation written in the form

$$f_a(\epsilon) = \int_0^\infty T(\epsilon, \epsilon') f_a(\epsilon') d\epsilon', \quad (9)$$

where  $T(\epsilon, \epsilon') d\epsilon' d\epsilon$  is the probability that a particle starting out in the energy interval  $d\epsilon'$  after a collision will be scattered into the energy interval  $d\epsilon$  at the next collision. If the energy range is divided into discrete intervals, Eq. (9) becomes

$$f_a^m = T^{mn} f_a^n, \quad (10)$$

where  $f_a$  is a vector,  $T$  a matrix, and a summation over repeated indices is implied. In the conventional Monte Carlo method described by Boardman, Fawcett, and Rees,<sup>10</sup> the random walk of a single particle in momentum space is simulated on a computer using random numbers. From this path an estimate of the vector  $f_a$  is immediately obtained. An estimate of the matrix  $T$  is obtained if at each collision the scattering probabilities to various energy intervals are recorded. An improved estimate of  $f_a$  is given by the solution of the set of linear equations (10) using the estimate of  $T$ . If the electric field  $E$  is given a small increment  $\delta E$ , the linear change in Eq. (10) is

$$\delta f_a^m = T^{mn} \delta f_a^n + \delta T^{mn} f_a^n. \quad (11)$$

To solve for  $\delta f_a$  it is thus necessary to have an estimate of  $\delta T$ . This estimate can be obtained from the collision density

$$p(k, k_0) = \frac{\hbar \nu(k)}{eE} \exp\left(-\frac{\hbar}{eE} \int_{k_0}^k \nu(k) dk\right), \quad (12)$$

where  $p(k, k_0) dk$  is the probability that a particle starting out at wave number  $k_0$  will be scattered in the interval  $(k, k + dk)$ .  $\nu(k)$  is the collision frequency,  $k$  and  $k_0$  are wave numbers parallel to the electric field, and the transverse wave number is not written out explicitly for clarity. If the elec-

tric field is given a small increment  $\delta E$ , the linear change in the collision density is

$$\delta p(k, k_0) = \frac{\delta E}{E} p(k, k_0) \left( \frac{\hbar}{eE} \int_{k_0}^k \nu(k) dk - 1 \right), \quad (13)$$

but

$$\frac{\hbar}{eE} \int_{k_0}^k \nu(k) dk = \ln \frac{1}{\rho}, \quad (14)$$

where  $\rho$  is the random number used to generate the times of flight between collisions. Thus

$$\delta p(k, k_0) = \frac{\delta E}{E} p(k, k_0) \left( \ln \frac{1}{\rho} - 1 \right). \quad (15)$$

The matrix  $\delta T$  can thus be obtained if the probabilities used in the estimate of the matrix  $T$  are multiplied by  $\ln(1/\rho) - 1$  in the respective points of collision. In the same way differential changes in quantities like the average velocity and time of flight of particles starting out in each energy interval are obtained.

In a practical case  $\nu(k)$  is a very complicated function of energy. It is thus difficult to solve Eq. (14) for the times of flight. This problem is solved through the introduction of a "self-scattering" mechanism as described by Boardman, Fawcett, and Rees,<sup>10</sup> that is, an additional scattering process

$$S(\vec{k}, \vec{k}') = [\Gamma(\vec{k}) - \nu(\vec{k})] \delta(\vec{k} - \vec{k}'), \quad (16)$$

where  $\nu(\vec{k})$  is the total scattering rate of real scattering processes while  $\Gamma(\vec{k})$  is a simple function of  $\vec{k}$  and usually chosen to be a constant. In the case of *n*-type germanium, however, it was found to be more efficient to choose  $\Gamma$  as a piecewise constant function of energy. In the calculation of  $\delta p$  only real scattering events may be taken into account. This is done by multiplying the transition probabilities by  $\sum_n [\ln(1/\rho_n) - 1]$  in each point of real collision where the sum goes over all self-scattering events including the last real collision. A proof of this is given in Appendix A.

A second method to calculate differential quantities can be deduced from the Shockley-Chambers path integral formula. In the notation of Sec. II the Boltzmann equation is

$$\frac{eE}{\hbar} \frac{\partial f}{\partial k_L} = Lf - \nu f, \quad (17)$$

corresponding to the path integral formula<sup>9</sup>

$$f = \frac{\hbar}{eE} \int_{-\infty}^{k_L} Lf \exp\left(-\frac{\hbar}{eE} \int_z^{k_L} \nu(k) dk\right) dz. \quad (18)$$

If an increment  $\delta E$  is added to the electric field, the path integral formula for the change in the distribution function is

$$\delta f = \frac{\hbar}{eE} \int_{-\infty}^{k_L} \left( L\delta f + \frac{\delta E}{E} (\nu f - Lf) \right)$$

$$\times \exp\left(-\frac{\hbar}{eE} \int_z^{k_L} \nu(k) dk\right) dz. \quad (19)$$

In terms of synchronous ensembles,

$$\frac{\delta E}{E} (\nu f - Lf) = \frac{\delta E}{E} (f_b - f_a), \quad (20)$$

where  $f_b$  is the "before-scattering" ensemble. This can be interpreted as a source generating both "positive" and "negative" particles which are continuously scattered and annihilated. In terms of after-scattering ensembles, Eq. (19) is given by

$$\delta f_a^m = T^{mn} \delta f_a^m + (\delta E/E) (g_a^m - f_a^m), \quad (21)$$

where  $g_a$  is the distribution of particles after their first collision if they start out from the distribution  $f_b$ . It can be generated during the Monte Carlo calculation if a new particle is generated in each point of real collision and is subsequently followed through its first real collision. This procedure also gives differential changes in quantities like the average time of flight. A proof of this is given in Appendix B.

Both methods described above are in principle exact. In the practical implementation on a computer, however, an error is introduced from the necessity to have a finite number of energy intervals. In the calculations to be described in Sec. IV the energy axis was divided into 100 intervals within the range where the particle density was appreciable. The precision was checked by changing the size of the intervals. This showed the error introduced by the finite size of the intervals to be negligible.

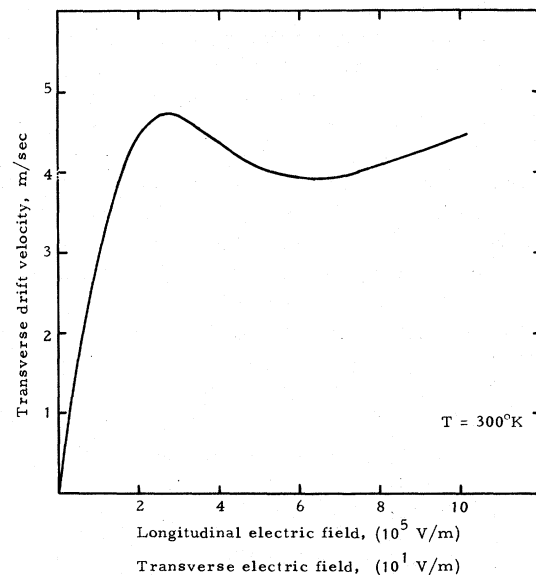


FIG. 2. Variation of the transverse drift velocity with field.

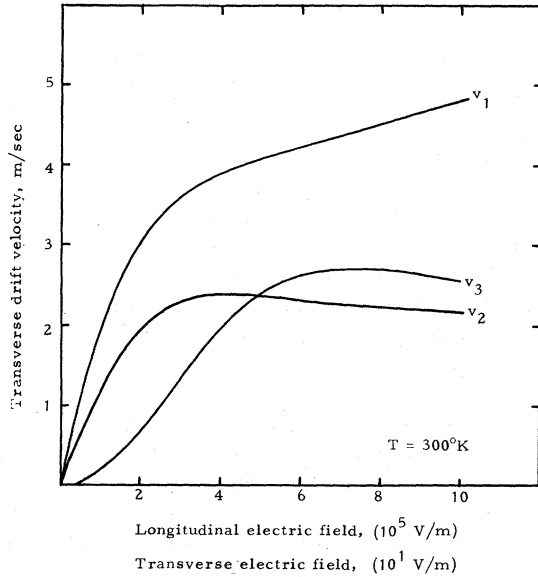


FIG. 3. Components of the transverse drift velocity versus electric field.

In the numerical calculations both methods were found to be useful. In the first method the random walk is simpler and requires less computer time for the same number of scattering events. The second method, on the other hand, requires less storage space since no matrix  $\delta T$  has to be stored. The statistical errors were found to be comparable although in a certain sense complementary; in a range of electric field where one method had a large error the other could give a small error.

The generalizations necessary for the solution of

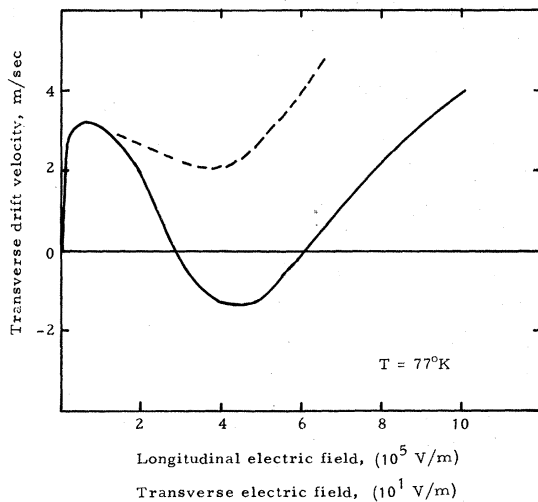


FIG. 4. Variation of the transverse drift velocity with field for a nonequivalent intervalley coupling constant equal to  $2.5 \times 10^{10}$  eV/m (dashed curve) and  $5 \times 10^{10}$  eV/m (solid curve).

Eq. (8) are few. With the model of the band structure and scattering processes used here each valley is isotropic and all scattering processes are velocity randomizing. The Monte Carlo calculation is done for a field in the [110] direction. From Eq. (8) it follows that it is only necessary to compute differential quantities in one of the sets of equivalent minima. This reduces the problem of the finite size of the energy intervals.

#### IV. NUMERICAL RESULTS

The transverse drift velocity versus longitudinal electric field is shown in Fig. 2 for a transverse field equal to  $10^{-4}$  times the longitudinal field as calculated for  $T = 300^\circ\text{K}$  and scattering parameters according to Table II. This choice of the transverse field corresponds to a constant angular deviation of the total field from the [110] direction. The three components of the drift velocity as described in Sec. II are given in Fig. 3.  $v_1$  is due to the change in the direction of the effective field in each valley,  $v_2$  is caused by the change in the magnitudes of the drift velocities in the  $\langle 111 \rangle$  and  $\langle \bar{1}\bar{1}\bar{1} \rangle$  minima, and  $v_3$  is obtained from the repopulation of carriers between these valleys.  $v_3$  is directed oppositely to  $v_1$  and  $v_2$  and has to be larger than the sum of  $v_1$  and  $v_2$  for an instability to occur. From Fig. 3 it is clear that this condition is not fulfilled. The repopulation is thus too small for an instability to occur in this case. Calculations have also been made for different values of the scattering parameters. No significant increase in the repopulation effect was

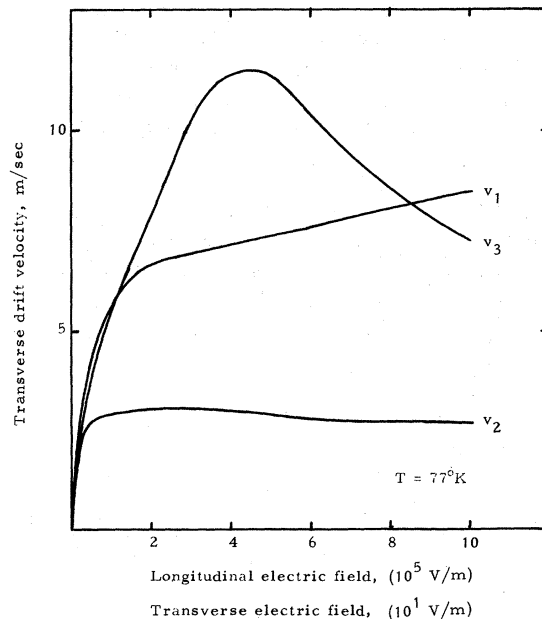


FIG. 5. Components of the transverse drift velocity vs electric field.

observed. If the model used is valid, it thus has to be concluded that the Erlbach instability does not exist at room temperature.

At 77°K the situation is different. Figures 4 and 5 show the results obtained at this temperature. A strong repopulation is obtained, and with the scattering parameters given in Table II the transverse resistance is negative for a longitudinal field in the range  $3-6 \times 10^5$  V/m. The instability is, however, very sensitive to the value of the coupling constant for nonequivalent intervalley scattering. It has to be larger than about  $4 \times 10^{10}$  eV/m for an instability to occur. The value of this parameter is not well established, although experimental measurements of the resistivity under hydrostatic pressure<sup>11</sup> indicate a value close to  $5 \times 10^{10}$  eV/m. Thus a transverse instability may very well exist at 77°K, and experimental measurements of the transverse mobility could provide a better understanding of the role of the  $\langle 100 \rangle$  minima in the conduction process in  $n$ -type germanium.

#### ACKNOWLEDGMENTS

The author would like to thank Dr. H. Kroemer for giving the impulse to start this work. He is

grateful to the National Bureau of Standards and the University of Colorado for their hospitality during the time when a part of this paper was prepared.

#### APPENDIX A

Proof that the average of  $\sum_n [\ln(1/\rho_n) - 1] \delta E/E$ , where the sum goes over all collisions up to the first real collision, will give  $\delta p(k, k_0)$ .

The total scattering frequency is

$$\gamma(k) = \nu(k) + \nu_s(k), \quad (\text{A1})$$

the sum of the real scattering frequency and the "self-scattering" frequency. The collision density of particles starting out at wave number  $k_0$  is

$$p_0(k, k_0) = \gamma(k) \exp\left[-\int_{k_0}^k \gamma(k) dk\right], \quad (\text{A2})$$

where  $\hbar/eE = 1$  is assumed. The collision density for a real scattering to occur in the first collision is

$$p_1(k, k_0) = [\nu(k)/\gamma(k)] p_0(k, k_0). \quad (\text{A3})$$

The collision density for the first real collision to occur in the  $(n+1)$ st collision is

$$\begin{aligned} p_{n+1}(k, k_0) &= \frac{\nu(k)}{\gamma(k)} \int_{k_0}^k dk_n p_0(k, k_n) \frac{\nu_s(k_n)}{\gamma(k_n)} \int_{k_0}^{k_n} dk_{n-1} p_0(k_{n-1}, k_{n-1}) \cdots \frac{\nu_s(k_2)}{\gamma(k_2)} \int_{k_0}^{k_2} p_0(k_2, k_1) \frac{\nu_s(k_1)}{\gamma(k_1)} p_0(k_1, k_0) dk_1 \\ &= \frac{\nu(k)}{\gamma(k)} p_0(k, k_0) \int_{k_0}^k dk_n \nu_s(k_n) \int_{k_0}^{k_n} dk_{n-1} \nu_s(k_{n-1}) \cdots \nu_s(k_2) \int_{k_0}^{k_2} \nu_s(k_1) dk_1. \end{aligned} \quad (\text{A4})$$

Using the symmetry of the integrands gives

$$p_{n+1}(k, k_0) = \frac{\nu(k)}{\gamma(k)} p_0(k, k_0) \frac{1}{n!} \int_{k_0}^k \nu_s(k_1) dk_1. \quad (\text{A5})$$

The distances between points of collision are generated by the random numbers

$$\int_{k_{m-1}}^{k_m} \gamma(k) dk = \ln \frac{1}{\rho_m}. \quad (\text{A6})$$

Thus

$$r_n = \sum_{i=1}^n \left( \ln \frac{1}{\rho_i} - 1 \right) = \int_{k_0}^k \gamma(k_1) dk_1 - n. \quad (\text{A7})$$

The average of  $r_n$  is thus

$$\begin{aligned} \langle r_n \rangle &= \sum_{n=1}^{\infty} r_n p_n(k, k_0) \\ &= \frac{\nu(k)}{\gamma(k)} p_0(k, k_0) \sum_{n=1}^{\infty} \frac{1}{n-1!} \left( \int_{k_0}^k \gamma(k_1) dk_1 - n \right) \left( \int_{k_0}^k \nu_s(k_1) dk_1 \right)^{n-1} \\ &= \frac{\nu(k)}{\gamma(k)} p_0(k, k_0) \left( \int_{k_0}^k \gamma(k_1) dk_1 - \int_{k_0}^k \nu_s(k_1) dk_1 - 1 \right) \exp\left( \int_{k_0}^k \nu_s(k_1) dk_1 \right) \end{aligned}$$

$$= p(k, k_0) \left( \int_{k_0}^k \nu(k_1) dk_1 - 1 \right) = \delta p(k, k_0). \quad (\text{A8})$$

Q. E. D.

#### APPENDIX B

Proof that the change in the collision density caused by an increase  $\delta E$  in the electric field is equal to the density of "second" collisions minus the density of first collisions times the fractional change in the field is as follows.

The collision density at wave number  $k$  of particles starting out at  $k_0$  is

$$p(k, k_0) = \frac{\hbar \nu(k)}{eE} \exp\left(-\frac{\hbar}{eE} \int_{k_0}^k \nu(k) dk\right). \quad (\text{B1})$$

The change in the collision density caused by the field  $\delta E$  is

$$\delta p(k, k_0) = \frac{\delta E}{E} p(k, k_0) \left( \frac{\hbar}{eE} \int_{k_0}^k \nu(k) dk - 1 \right). \quad (\text{B2})$$

The density of "second" collision is obtained if particles start out from the density  $p(k, k_0)$ . Thus

$$\begin{aligned} p_2(k, k_0) &= \int_{k_0}^k p(k, k_1) p(k_1, k_0) dk_1 \\ &= p(k, k_0) \frac{\hbar}{eE} \int_{k_0}^k \nu(k) dk \end{aligned} \quad (\text{B3})$$

and

$$\begin{aligned} \frac{\delta E}{E} [p_2(k, k_0) - p(k, k_0)] \\ &= \frac{\delta E}{E} p(k, k_0) \left( \frac{\hbar}{eE} \int_{k_0}^k \nu(k) dk - 1 \right) \\ &= \delta p(k, k_0). \end{aligned} \quad (\text{B4})$$

Q. E. D.

<sup>1</sup>E. Erlbach, Phys. Rev. **132**, 1976 (1963).

<sup>2</sup>M. Shyam and H. Kroemer, Appl. Phys. Letters **12**, 283 (1968).

<sup>3</sup>E. G. S. Paige, IBM J. Res. Develop. **13**, 562 (1969).

<sup>4</sup>C. Hammar, Phys. Rev. B **4**, 417 (1971).

<sup>5</sup>E. M. Conwell, in *Solid State Physics*, edited by F. Seitz and D. Turnbull (Academic, New York, 1967), Suppl. 9.

<sup>6</sup>C. Herring and E. Vogt, Phys. Rev. **101**, 944 (1956).

<sup>7</sup>This separation of the components is different from the one used by Erlbach (Ref. 1). Here  $\delta j_b$  is determined by the differential mobility in the  $\langle 111 \rangle$  and  $\langle 11\bar{1} \rangle$  valleys. The differential mobility  $d\nu^*/dE^*$  can be written as  $\mu_0^* + (d\mu_0^*/dE^*)E^*$ , where  $\mu_0^*$  is the total mobility in the transformed system. Erlbach included the first, positive term in his current  $\delta j_1$  and defined his current  $\delta j_2$  as due

to the second, negative term. In the range of fields and temperatures studied here, the differential mobility was everywhere found to be positive. Thus the current  $\delta j_b$  and the current  $\delta j_2$  in Erlbach's paper are in opposite directions.

<sup>8</sup>W. Fawcett, A. D. Boardman, and S. Swain, J. Phys. Chem. Solids **31**, 1963 (1970).

<sup>9</sup>P. J. Price, in *Proceedings of the Ninth International Conference on the Physics of Semiconductors*, edited by S. M. Ryvkin (Nauka, Leningrad, 1968), p. 753.

<sup>10</sup>A. D. Boardman, W. Fawcett, and H. D. Rees, Solid State Commun. **6**, 305 (1968).

<sup>11</sup>A. Jayaraman and B. B. Kosicki, in *Proceedings of the Ninth International Conference on Semiconductors*, edited by S. M. Ryvkin (Nauka, Leningrad, 1968), p. 53.